2014 IEEE International Conference on Robotics & Automation (ICRA)
Hong Kong Convention and Exhibition Center
May 31 - June 7, 2014. Hong Kong, China

Modeling of a carangiform-like robotic fish for both forward and backward swimming: based on the fixed point*

Liang Li[1] Chen Wang[1,2] and Guangming Xie [1]

***Abstract*— In this paper, a dynamic model is proposed for a carangiform-like robotic fish swimming both forwards and backwards. The robotic fish, which consists of a streamlined head, a flexible body and a caudal fin, is able to propel itself by generating a traveling propulsive wave traversing its body. We first modify the classical body wave function suggested by Lighthill to fit our robotic fish. Then we naturally define the point on fish's body which never undulates during swimming straight as "Fixed-point" and prove its existence and uniqueness. Using the property of the Fixed-point, we propose a model for our robotic fish and further investigate how the swimming speed is affected by the position of the unique Fixed-point. It is found that the robotic fish achieves its maximum speed of swimming forwards and backwards when the Fixed-point located on the head and the tail, respectively. Finally, we apply the proposed model combining with a CPG-based locomotion controller to the real robotic fish. Both simulations and experiments show that the proposed model is capable to predict the speed of the robotic fish.**

I. INTRODUCTION

Organisms have probably existed in the world for hundreds of millions of years. Their perfect physical structures and excellent locomotion properties emerging from the continuous long-period evolution fascinate all researches who hope to design better mobile robots. Among all kinds of aquatic organisms, fish are always paid more attention to and often imitated to design underwater robots due to its outstanding locomotion skills [1], [2], [3], [4], [5].

Increasing studies on dynamic models of both real fish and robotic fish offer researchers an unprecedented opportunity to design better fish-like robots. Lighthill has proposed a dynamic model named Elognated Body Theory (EBT)[6] for both anguilliform and carangiform fish. In the EBT, Lighthill have derived mean speed and thrust of fish by input body wave. Yu et al. have bulit a swimming model for a multijoint robotic fish based on Lagrange theory [7]. By solving the Navier-Stokes equation, the hydrodynamic force distribution can be computed based on computational fluid dynamics (CFD), and the speed of fish can thereby be derived [8]. Recently, Porfiri group have computed propulsion of fish tail from a 2-D mean velocity field got by digital particle image velocimetry (DPIV) [9] and investigated fish swimming ability by vibration model using the classical Euler-Bernoulli beam theory [10]. Most research efforts made on the carangiform fish-like robots have focused on the forward swimming under the assumption that the front of the fish, especially its head, has no oscillation. However, in some harsh environments such as narrow gaps and pipelines, the robots are required to swim backwards by shaking their heads.

In this paper, we propose a dynamic model for a carangiform-like robotic fish which incorporates both forward and backward swimming. The robotic fish that we have developed can generate a propulsive wave that travels along its body to propel itself. Based on Lighthill's Elongated Body Theory, we modify the classical body wave function to fit our robotic fish. We observed that there exists a point on fish's body that never undulates during swimming straight. We prove the existence and uniqueness of such a point and naturally call it "Fixed-point". Using the property of the Fixed-point, we arrive at a model for the fish-like robot, in which the mean speed of bi-direction swimming is derived by the modified body wave equation. It is found that the forward speed decreases to zero and then the backward speed increases when the fixed-point moves from the head to the tail. In other words, the robotic fish achieves its maximum forward and backward speed when the Fixed-point is on the head and the tail, respectively. Finally, combined with a CPG-based (Central Pattern Generator) locomotion controller, our proposed model is applied to the real robotic fish. It is shown from the experiments that the proposed model is capable to predict the speed of the robotic fish.

The remainder of the paper is organized as follows. In Section II, we present the prototype of of a carangiform robotic fish. Then a dynamic model of the robotic fish is proposed for both forward and backward swimming in Section III. In Section IV, we apply our model combining with a CPG-based locomotion controller to the real robotic fish. The experiments results are shown in Section V.

II. DESCRIPTION OF CARANGIFORM FISH-LIKE ROBOT

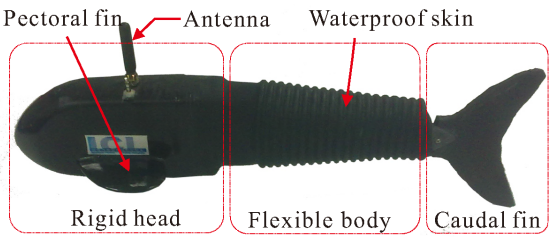

Fig. 1. Prototype of the robotic fish

*This work was supported by the National Natural Science Foundation of China (NSFC, No. 60774089, 10972003).

[1] L. Li, C. Wang and G. Xie are with the Intelligent Control Laboratory, College of Engineering, Peking University, Beijing, China (E-mail: {liatli, wangchen, xiegming}@pku.edu.cn)

[2] C. Wang is also with the Faculty of Mathematics and Natural Sciences, ITM, University of Groningen, the Netherlands

The fish-like robot that we have developed is shown in Fig. 1, which consists of three parts: a rigid head, a flexible body and a caudal fin [11]. The rigid head accommodates a control unit, a wireless communication module and a set of batteries. The batteries are placed at the bottom of the head to ensure the vertical stability of the robot during swimming. A pair of pectoral fins is fixed on both side of the head to ensure the roll stability. The flexible body is composed of three joints. Each joint is connected to a servomotor, which is used to adjust the deflection angle of this joint. The rubber caudal fin is fixed on the third joint. To be waterproof, the robot is covered by a rubber tube from head to tail. The robotic fish is about 40cm in length and 900g in weight. The density of the robot is designed to be just a little smaller than that of the water to make the robot swimming just below the water surface.

III. Model

In this section, we first give a description of the body wave and review Lighthill's Elongated Body Theory. Based on these, we introduce a definition of Fixed-point and prove its existence and uniqueness. Then we are able to propose a model of speed for both forward and backward swimming. We further investigate how the swimming speed is affected by the position of the unique Fixed-point.

A. Description of Body Wave

In nature, most fishes generate thrust through body undulating to overcome the drag of water, and these were first observed in the studies of James Gray [12]. To describe how fish body undulates periodically, a mathematical body wave function is established. Fig. 2 gives a top view of

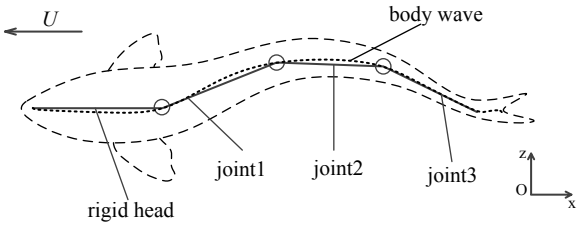

Fig. 2. Top view of fish body wave defined in the earth-fixed inertial reference frame.

carangiform fish body in the Earth-fixed inertial reference frame (x,z). Fish swims along the negative direction of x, and its perpendicular displacement is described as $z(x,t)$. Lighthill advised one expression of the body wave as

$$z(x,t) = \left(c_1 x + c_2 x^2\right)\sin(kx+\omega t) \tag{1}$$

where $z(x,t)$ denotes transverse displacement of body, x is the displacement along main axis, k is expressed as $2\pi/\lambda$ where λ is body wave length, c_1 and c_2 are linear and quadratic wave amplitude envelopes respectively, ω is regarded as frequency of body wave. All these parameters are body wave parameters that determines undulation of fish body.

B. Lighthill's Elongated Body Theory

Elongated Body Theory was first proposed by Lighthill in 1960 [6], and has been widely used in the hydrodynamic analysis of modes of locomotion and propulsive efficiency of elongated fishes [13]. When thrust balances drag force, fish reaches a steady state with a mean speed U. And the wold "mean" refers to the average over one period of fish body undulation. According to Lightill's Elongated Body Theory, we get the mean thrust described as [6]

$$\overline{T} = \left[\frac{1}{2}\rho A(x)\left(\overline{\left(\frac{\partial z(x,t)}{\partial t}\right)^2} - U^2\overline{\left(\frac{\partial z(x,t)}{\partial x}\right)^2}\right)\right]_{x=l} \tag{2}$$

where $\overline{(\cdot)}$ denotes the mean value, ρ is the density of fluid, l denotes the length of fish and $A(x)$ has the dimensions of area, calculated as

$$A(x) = \frac{1}{4}\pi S_c^2 \tag{3}$$

where S_c is the width of tail fin. Besides, in hydromechanics, $1/4\rho\pi S_c^2$ is defined as virtual mass m [14]. Under inviscid flow condition, drag force of a fish is experimentally expressed as

$$D = \frac{C_D \rho U^2 S}{2} \tag{4}$$

where C_D is a coefficient determined by experiments, and S is the wetted surface area of the undulation part.

After fish reaches the balance of thrust and drag force, we get the calculation of speed U as

$$U = \left[\sqrt{\frac{m\overline{\left(\frac{\partial z(x,t)}{\partial t}\right)^2}}{C_D\rho S + m\overline{\left(\frac{\partial z(x,t)}{\partial x}\right)^2}}}\right]_{x=l} \tag{5}$$

C. Model of Fish Speed for Bi-directional Swimming

In Lighthill's Elongated Body Theory, the rigid head is assumed to have no displacement in z axial. Therefore, $A(0)$ is zero and fish head generates no thrust. However, robotic fish, in real experience, usually oscillates its head and sometimes with large amplitude, and thus $A(0) \neq 0$. Then fish speed is generated by the resultant force of head and tail oscillating thrust.

Although both head and tail of robotic fish have oscillations during fish swimming, we find there is still one point in the swimming robotic fish that always has no undulation at anytime if all the parameters are taken as the same. We called this point as Fixed-point (FP), and based on it we redescribed the body wave function as

$$z'(x,t) = (c_1(x-x_0) + c_2(x^2 - x_0^2))\sin(k(x-x_0)+\omega t) \tag{6}$$

where x_0 denotes the coordinate of FP in x axis. Fig. 3 depicts sets of periodic body waves with different FPs. We can find that although parameters in body wave function are the same, the shapes of body wave are quietly different with various FPs.

Once fish movements are described by this body wave function, propulsion generated by body undulation can be

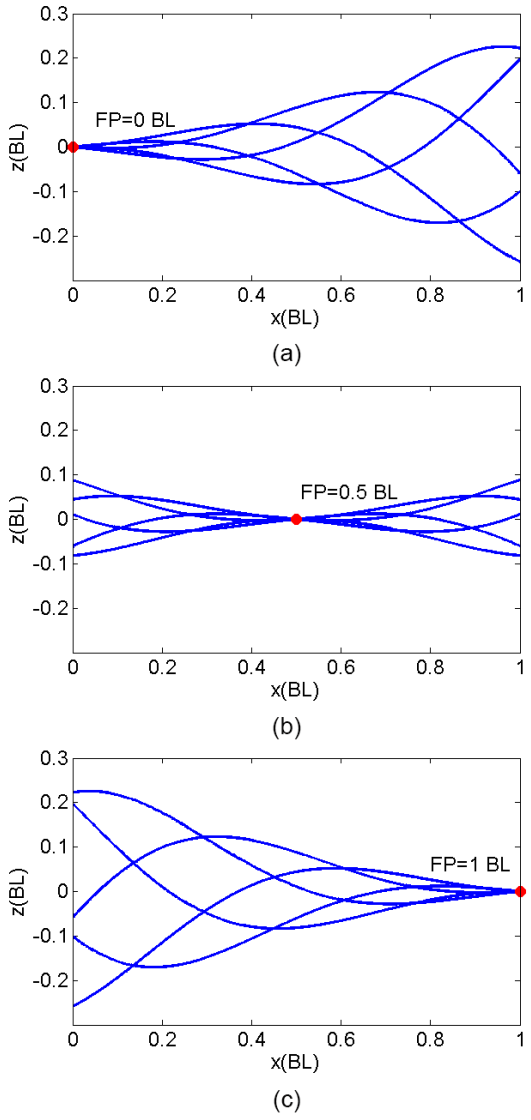

Fig. 3. Body wave curves with FP at (a) 0 BL (b) 0.5 BL (c) 1 BL, while other parameters keep the same.

divided into two parts: front part described in (7) and rear part denoted in (8). Its front and rear virtual masses are recorded as m_1 and m_2, and thrusts generated by these two parts are calculated in vector (the positive direction is from head to tail),

$$\overline{T_1} = \left[\frac{m_1}{2}\left(\overline{\left(\frac{\partial z'(x,t)}{\partial t}\right)^2} - U^2\overline{\left(\frac{\partial z'(x,t)}{\partial x}\right)^2}\right)\right]_{x=0} \quad (7)$$

$$\overline{T_2} = -\left[\frac{m_2}{2}\left(\overline{\left(\frac{\partial z'(x,t)}{\partial t}\right)^2} - U^2\overline{\left(\frac{\partial z'(x,t)}{\partial x}\right)^2}\right)\right]_{x=l}. \quad (8)$$

If the resultant thrust $(\overline{T_1}+\overline{T_2})$is negative, robotic fish will swim forward and its speed is calculated as

$$U = -\sqrt{\frac{m_1\left\{\overline{\left(\frac{\partial z'}{\partial t}\right)^2}\right\}_{x=0} - m_2\left\{\overline{\left(\frac{\partial z'}{\partial t}\right)^2}\right\}_{x=l}}{C_D\rho S + m_1\left\{\overline{\left(\frac{\partial z'}{\partial x}\right)^2}\right\}_{x=0} - m_2\left\{\overline{\left(\frac{\partial z_2}{\partial x}\right)^2}\right\}_{x=l}}}. \quad (9)$$

However, if the resultant thrust is positive, robotic fish will swim backward and the speed is derived as

$$U = \sqrt{\frac{m_1\left\{\overline{\left(\frac{\partial z'}{\partial t}\right)^2}\right\}_{x=0} - m_2\left\{\overline{\left(\frac{\partial z'}{\partial t}\right)^2}\right\}_{x=l}}{-C_D\rho S + m_1\left\{\overline{\left(\frac{\partial z'}{\partial x}\right)^2}\right\}_{x=0} - m_2\left\{\overline{\left(\frac{\partial z'}{\partial x}\right)^2}\right\}_{x=l}}}. \quad (10)$$

One more attention, with some body wave parameters, both (9) and (10) have no solution. One explanation proposed by Lighthill is that the thrust generated by robotic fish is so small that it needs an external thrust to push it against its drag [6].

D. Existence and uniqueness of FP

Since in the body wave equation (6) FP is assumed to extend between $0 \le x_0 \le l$, FP must exist in fish body. And the displacement in z direction is identically vanishing at any time t. We get the uniqueness of FP by reductio as absurdum. One first assume there exits another FP (x_0') in fish body, and $x_0' \neq x_0$, then we get

$$(c_1(x_0' - x_0) + c_2(x_0'^2 - x_0^2))\sin(k(x_0' - x_0) + \omega t) = 0 \quad (11)$$

Since time t varies, values of $sin(k(x_0' - x_0) + \omega t)$ is not identically vanishing. Because parameters c_1 and c_2 are not zero, x_0' equals x_0 and FP is unique.

E. Simulation of Thrust and Speed vs. FP

Fig. 4 and Fig. 5 respectively show a simulation of thrust and speed of FP, in which parameters are set as shown in Table. I. Driven by the same body wave function, fish gets maximum forward and backward speeds as FP respectively stays in the head and tail of fish. Moreover, there exits one point ($x_t = 0.735\ BL$ described in Fig. 4 and Fig. 5) in fish body, which leads the resultant thrust equals zero. That is to say, under this FP, fish struggles in the water without speed. This situation is always happened during our experiments with robotic fish. Because the asymmetry of virtual mass in fish head (m_1) and tail (m_2), maximum backward speed (0.89 BL/s) is lower than forward ($-1.07\ BL/s$). For a robotic fish, the location of FP is determined by both body wave function and mechanical-structural design. Usually, it is more difficult to modify mechanical-structure of robot than body wave function (controlled by software). Therefore, in real robots, FPs are usually adjusted through body wave functions for maximum forward and backward speed.

TABLE I

PARAMETERS SETTING IN SIMULATION

Variable	Value
c_1	0.2489
c_2	0.5173 (m^{-1})
k	2.938 (rad/m)
ω	1.4 (rad/s)
l	0.4 (m)
S	0.28 (m)
S_c	0.032 (m)
ρ	1000 (kg/m^3)
$m1$	61.575 (g)
$m2$	12.315 (g)
C_D	0.1309

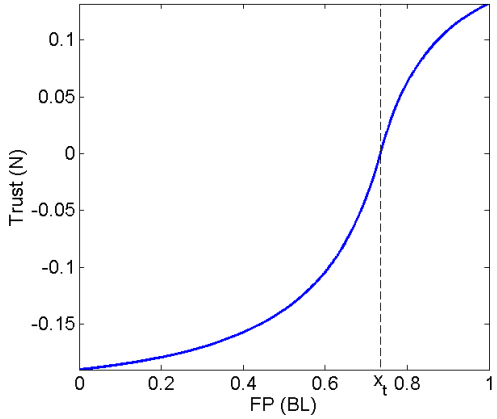

Fig. 4. Thrust of fish vs. FP in fish body

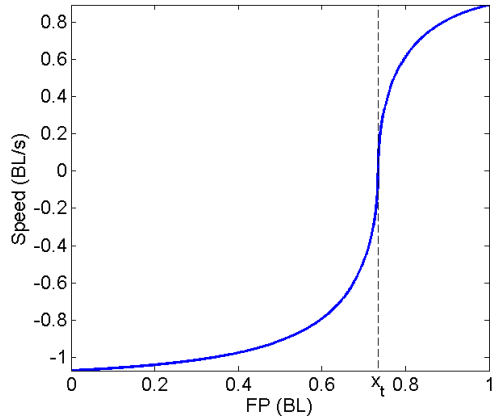

Fig. 5. Speed of fish vs. FP in fish body

IV. CPG-BASED LOCOMOTION CONTROLLER

This section aims to apply the model we proposed in the previous section to a real robotic fish. To achieve this goal, we first introduce the CPG-based locomotion controller embedded in our robotic fish. Then the transition between CPG parameters and body wave parameters is given.

A. CPG-based Controller

CPG was found in animals, especially in vertebrates, and first proposed by T G Brown in 1914 [15]. Since then various artificial CPG controllers are built. In contrast to traditional locomotion controllers, CPG is a non model based controller. Due to its wonderful properties, engineers transplant this locomotion control method to the field of robot through kinds of mathematic models [16], [17], [18]. For instance, the coupled oscillator model, a simple and popular CPG controller, was first proposed by Ijspeert to verify the neural CPG in salamander [18].

A simple, linear, yet still powerful CPG model is proposed for the control of our robotic fish [19]. This CPG controller is also based on coupled oscillators that is similar with neural networks in animals. This model is defined as:

$$\ddot{r}_i(t) = \alpha\left[\alpha\left(R_i - r_i(t)\right) - 2\dot{r}_i(t)\right] \tag{12}$$

$$\ddot{\phi}_i(t) = \sum_{j=1, j\neq i}^{N} \mu\left[\mu\left(\phi_j(t) - \phi_i(t) - \varphi_{ij}\right) - 2\left(\dot{\phi}_i(t) - 2\pi v_i\right)\right] \tag{13}$$

$$\theta_i(t) = r_i(t)\cos\left(\phi_i(t)\right), \tag{14}$$

where r_i, ϕ_i and θ_i represent the amplitude, the offset, the phase and the outputs of *ith* oscillator respectively. R_i denotes the amplitude of ith oscillator that determines body wave shape of robotic fish. φ_{ij} calculated by $\phi_j - \phi_i$ means a base of phase between oscillator i and j when the oscillators reach stability. And v is the frequency of all the oscillators. Structural parameters α, β and μ respectively affect the convergence rate of r_i and ϕ_i. Moreover, because φ_{ij} equals $-\varphi_{ji}$ and $\varphi_{ij} = \varphi_{ik} + \varphi_{kj}$ in real robots, two phase biases, such as φ_{12} and φ_{13}, can describe all the phase relationships of three oscillators.

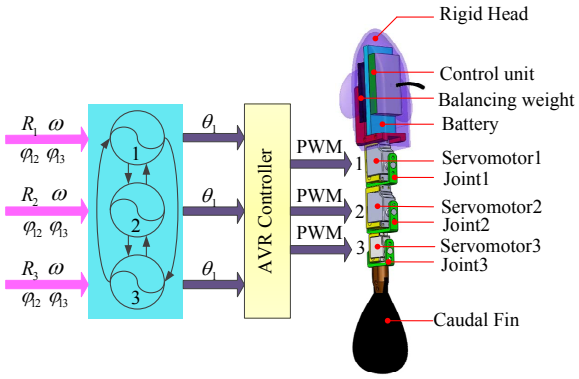

Fig. 6. Framework of CPG controller embedded in the three-joints robotic fish

This CPG model is designed as linear so that it can be easily implemented in microcontrollers on board in robots. Fig. 6 shows a framework of the application of the above CPG controller in our robotic fish. All the parameters are received from upper computer, After received parameters from upper computer, microcontroller in robotic fish first

generates output angles through CPG network and then transform these angles to PWM signals to drive servomotors.

B. Transition between CPG parameters and body wave parameters

In the model we proposed, fish swimming speed is derived by body wave function, while real robot is controlled by CPG parameters (R_i, φ_{ij} and v). Therefore, transition from body wave parameters to CPG controller is needed. Since our robot is composed of four hinge joints (one head and three joints), body wave curve is fitting with five points (x_i, z_i) satisfying

$$z(x_i,t) = \left(c_1 x_i + c_2 x_i^2\right)\sin(kx_i + \omega t) \tag{15}$$

The transition between body wave parameters and CPG parameters can be described as:

$$\begin{aligned} R_1 &= c_1 x_2 + c_2 x_2^2 && (16)\\ R_2 &= c_1 x_3 + c_2 x_3^2 && (17)\\ R_3 &= c_1 x_4 + c_2 x_4^2 && (18)\\ \varphi_{12} &= k x_3 && (19)\\ \varphi_{13} &= k x_4 && (20)\\ v &= \frac{2\pi}{\omega} && (21) \end{aligned}$$

V. Experimental Verification

In this section, we first introduce the experimental apparatus and then describe experimental results verifying the effectiveness of our model.

A. Experimental Research Apparatus

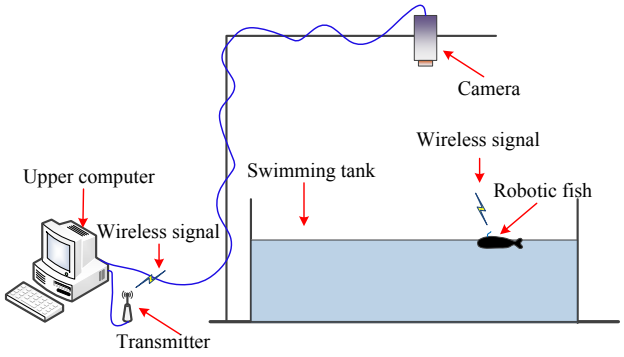

Fig. 7. Experimental validation apparatus for model validation

The hardware testbed for model validation consists of four parts: an upper computer, a wireless transmitter, a global view camera and a swimming tank (see Fig.7). This swimming tank is 300×200 *cm* with water height about 20 *cm*. A global view camera is equipped above the swimming tank to gain the videos with a resolution of 1920×1080 pixels and a depth of 8 b per pixel in real-time. In order to catch the details of body wave of fish, the recorded field by camera is defined as 50×90 *cm*. After input body wave parameters to upper computer, CPG parameters are calculated and sent to robotic fish. Videos of fish motion are captured by camera and stored in upper computer. FPs are analysed by PhotoShop with the videos. Once FP is acquired, along with body wave parameters, speed of fish including direction and value can be calculated. And the comparative analysis can be applied between simulating and experimental results.

B. Experimental Results

Since the mechanical-structure of robot can hardly be changed, we can adjust body wave parameters such as frequency and amplitudes to acquire different FPs. Based on our previous work about this robotic fish, we find there is a positive correlation between forward swimming speed and frequency. Therefore, we acquired different FPs by modifying frequency when fish swimming forward. And referenced to researches of backward swimming in nature, we also find two groups of body wave parameters that lead fish swim backward.

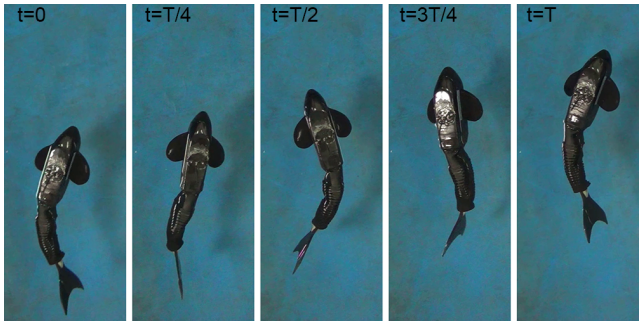

Fig. 8. Comparison of body wave shape for forward swimming with speed of 0.084 BL/s in one period $T = 5$ s

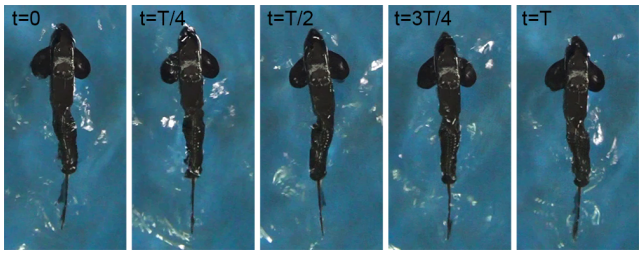

Fig. 9. Comparison of body wave shape for backward swimming with speed of 0.3 BL/s in one period $T = 0.4$ s

The capability of the model in predicting bi-directional speed was verified for different body wave inputs. CPG parameters were transferred by body wave parameters with the method described in Section IV. The FP extraction from video frames contains two main steps: 1) extract five images for each swimming modal from the videos in one period. 2) analysis and calculate speed and FP by comparison of fish locations within these figures. Due to the space limitation, we show two comparisons of swimming locomotion respectively for forward swimming with input body wave:

$$\begin{aligned} z(x,t) &= (0.2489(x-0.12) + 0.5173(x^2 - 0.12^2)) \\ &\quad \times \sin(2.938(x-0.12) + 31.4t) \end{aligned} \tag{22}$$

and backward swimming with input body wave:

$$z(x,t) = (-0.6339(x-0.4)+0.4597(x^2-0.4^2)) \times \sin(-9(x-0.4)+2.1t) \quad (23)$$

see Fig. 8 and Fig. 9. And for the other experiments of fish locomotion, readers may refer to the attached videos as supplementary material.

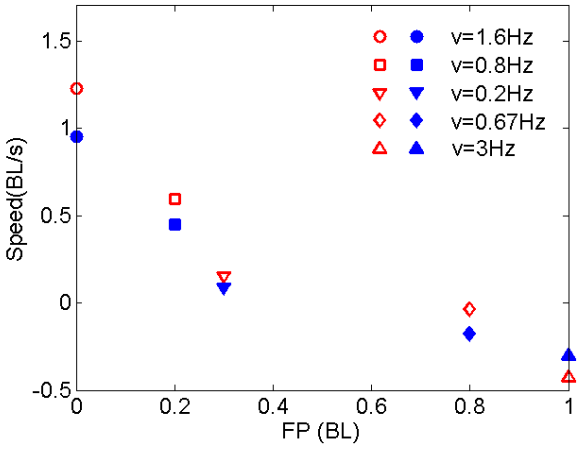

Fig. 10. Comparison of simulated and experiments at the same FP with same body wave, all the filled marks represents results of experiments and all the open markers denotes results of simulations

Simulations that take the same parameters measured from the physical robot have also been done for the comparison and validation. Five different body waves were investigated, and the simulated speeds of robotic fish match the experimental data well, as shown in Fig. 10. For the forward swimming in robotic fish, the achieved speed decreased as FP moved from head to body. While FP moves to the tail fish swam backward with maximum speed. Thus, For a robotic fish under special body wave input, maximum forward and backward swimming speed are acquired when FPs are in the head and tail, respectively. This gives us a guide for maximum robotic fish swimming speed including directions of both forward and backward.

VI. Conclusion

In this paper, we have presented a dynamic model for a carangiform fish-like robot, which described both forward and backward swimming. Based on the classical body wave function suggested by Lighthill, we have redescribed body wave function since the robotic fish swims with head shaking. One point in fish body that has no undulation while fish swimming in straight line was found and naturally defined as "Fixed-point". The problems of existence and uniqueness of FP have been discussed. Using this proposed model, we got the mean thrust and speed of fish by input FP-based body wave. Through simulations, we found the carangiform fish gets its maximum forward speed and maximum backward speed when the FP is in the head and the tail, respectively. We applied this FP theory to a CPG-controller embedded carangiform fish-like robot. Experiments with five body waves showed that the proposed model is capable to predict the speed of the underwater robot and validated the maximum bi-direction speed prediction.

This FP based dynamic model can be used in a wide range of optimization of forward or backward speed as a controller design guideline. Future work will include the derivation of FP by mechanical features and body wave function and further explore the effects between FP and mechanical structure. An extension of this study will comprise turning motion to consummate the motions of fish in 2D plane.

References

[1] J. M. Anderson, "vorticity control for efficient propulsion," Ph.D. dissertation, Massachusetts Ins. Technol/Woods Hole Oceanographic Inst. Joint Program, Woods Hole, MA, 1996.

[2] J. Yu, L. Wang, and T. Min, "A framework for biomimetic robot fish's design and its realization," in *Proc. Amer. Control Conf.*, Portland, USA, 2005, pp. 1593–1598 vol. 3.

[3] H. Hu, J. Liu, I. Dukes, and G. Francis, "Design of 3d swim patterns for autonomous robotic fish," in *Proc. 2006 IEEE/RSJ Int. Conf. on Intell. Robots and Syst*, Beijing, China, 2006, pp. 2406–2411.

[4] G. V. Lauder and E. G. Drucker, "Morphology and experimental hydrodynamics of fish fin control surfaces," *IEEE J. Ocean. Eng.*, vol. 29, no. 3, pp. 556–571, 2004.

[5] P. W. Webb, "Maneuverability - general issues," *IEEE J. Ocean. Eng.*, vol. 29, no. 3, pp. 547–555, 2004.

[6] M. J. Lighthill, "Note on the swimming of slender fish," *J. Fluid. Mech*, vol. 9, no. 02, pp. 305–317, 1960.

[7] J. Yu, M. Wang, Z. Su, M. Tan, and J. Zhang, "Dynamic modeling of a CPG-governed multijoint robotic fish," *Adv. Robotics*, pp. 1–11, 2013.

[8] T. L. DANIEL, "Unsteady aspects of aquatic locomotion," *Amer. Zool.*, vol. 24, no. 1, pp. 121–134, 1984.

[9] S. D. Peterson, M. Porfiri, and A. Rovardi, "A particle image velocimetry study of vibrating ionic polymer metal composites in aqueous environments," *IEEE/ASME Trans. Mechatronics*, vol. 14, no. 4, pp. 474–483, 2009.

[10] V. Kopman and M. Porfiri, "Design, modeling, and characterization of a miniature robotic fish for research and education in biomimetics and bioinspiration," *IEEE/ASME Trans. Mechatronics*, vol. 18, no. 2, pp. 471–483, 2013.

[11] J. Shao, L. Wang, and J. Yu, "Development of an artificial fish-like robot and its application in cooperative transportation," *Control Eng. Pract.*, vol. 16, no. 5, pp. 569–584, 2008.

[12] J. Gray, "Studies in animal locomotion I. the movement of fish with special reference to the eel," *J. Exp. Biol.*, vol. 10, no. 1, pp. 88–104, 1933.

[13] J. A. Sparenberg, "Survey of the mathematical theory of fish locomotion," *J. Eng. Mathematics*, vol. 44, no. 4, pp. 395–448, 2002.

[14] Z. Chen, S. Shatara, and X. Tan, "Modeling of biomimetic robotic fish propelled by an ionic polymer-metal composite caudal fin," *IEEE/ASME Trans. Mechatronics*, vol. 15, no. 3, pp. 448–459, 2010.

[15] T. G. Brown, "On the nature of the fundamental activity of the nervous centres; together with an analysis of the conditioning of rhythmic activity in progression, and a theory of the evolution of function in the nervous system," *J. Physiol.*, vol. 48, no. 1, pp. 18–46, 1914.

[16] P. Arena, "The central pattern generator: a paradigm for artificial locomotion," *Soft Computing*, vol. 4, no. 4, pp. 251–266, 2000.

[17] M. Okada, K. Tatani, and Y. Nakamura, "Polynomial design of the nonlinear dynamics for the brain-like information processing of whole body motion," in *Proc. IEEE Int. Conf. Robot. Autom.*, 2002, pp. 1410–1415.

[18] A. J. Ijspeert, A. Crespi, D. Ryczko, and J.-M. Cabelguen, "From swimming to walking with a salamander robot driven by a spinal cord model," *Science*, vol. 315, no. 5817, pp. 1416–1420, 2007.

[19] C. Wang, G. M. Xie, L. Wang, and M. Cao, "CPG-based locomotion control of a robotic fish: using linear oscillators and reducing control parameters via PSO," *Int. J. Innov. Comput. I.*, vol. 7, no. 7B, pp. 4237–4249, 2011.